6p

CONTROL OF OSCILLATORY THERMOCAPILLARY CONVECTION IN MICROGRAVITY

G. Paul Neitzel
The George W. Woodruff School of Mechanical Engineering
Georgia Institute of Technology
Atlanta, Georgia 30332-0405

ABSTRACT

Laboratory and numerical experiments are underway to generate, and subsequently suppress, oscillatory thermocapillary convection in a thin layer of silicone oil. The laboratory experiments have succeeded in characterizing the flow state in a limited range of Bond number—Marangoni number space of interest, identifying states of: *i*) steady, unicellular, thermocapillary convection; *i*) steady, multicellular, thermocapillary convection; and *iii*) oscillatory thermocapillary convection. Comparisons between experimental results and stability computations for a related basic state will be made.

INTRODUCTION

Thermocapillary convection is that motion induced in liquids with interfaces by a thermally induced interfacial-tension gradient. In the cases considered in this study, the interface will be a free surface between a liquid and gas and the surface tension will be a decreasing function of temperature, so that thermocapillary-induced surface motion will be from hot to cold regions. Thermocapillary convection occupies an important place in microgravity fluid dynamics because its existence is not swamped or masked, as in some terrestrial situations, by a stronger convection driven by buoyancy, which is significantly diminished in microgravity. In certain terrestrial applications such as the growth of semiconductor material using the float-zone process, the *instability* of thermocapillary convection is known to degrade crystal quality (1). In this case, the transition is to an *oscillatory* state which, when coupled with solidification, leads to the appearance of undesirable striations in the resulting material.

The transition to oscillatory thermocapillary convection in models of the float-zone process has lead to a great deal of research in identifying regions of stability and instability in so-called "half-zone" models of the process (2-5). The determination of such regions may make it possible, in some applications, to avoid the transition to oscillatory thermocapillary convection by operating a process in a region of guaranteed stability. This is not always practical, or even possible, however, and it is this fact which motivates the present research. In a situation for which oscillatory thermocapillary convection is both present and undesirable, we seek a method for detecting and suppressing this mode of convection through exploitation of the instability mechanism.

As a model for this approach, we use the problem studied extensively by Smith and Davis (6, 7), namely, thermocapillary convection in a layer driven by an imposed lateral temperature gradient. Among the basic states considered by Smith and Davis was one called a "return-flow," which would exist in a container of finite extent. This state, shown in Fig. 1, consists of a surface flow from the hot wall to the cold one and a flow along the bottom in the reverse direction driven by a pressure gradient established to conserve mass. For fluids of moderate Prandtl number $\mathrm{Pr} = \nu/\kappa$, where ν is the kinematic viscosity and κ the thermal diffusivity, Smith and Davis found the preferred mode of instability to be in the form of a new instability they termed a "hydrothermal wave," which propagates obliquely with the dominant velocity component in the direction opposite to that of the basic-state free-surface motion. The mechanism behind the instability was described by Smith (7) and is driven by communication between the thermal disturbances on the free surface and those in the layer's interior. We shall attempt to suppress the oscillations by sensing and actively modifying the free-surface temperature distribution.

The project consists of both laboratory and numerical experiments. The laboratory experiments have succeeded in establishing a state of oscillatory thermocapillary convection; in addition, states of steady, multicellular convection are observed in certain regions of Marangoni number–Bond number space, where the dynamic Bond number Bo_D is defined to be $Bo_D = \rho g \beta d^2 / \gamma$, where ρ is the density, g is the gravitational acceleration, β is the coefficient of volumetric expansion, σ is the mean surface tension and $\gamma = -d\sigma / dT$ is the rate of decrease of surface tension with temperature. Preliminary numerical work was utilized to assist in the design of the laboratory apparatus; more sophisticated numerical modeling of the flow is just commencing and will be reported on at a later date. A modification to the Smith and Davis (6) theory has been made to include the presence of buoyancy absent in the earlier work. Comparisons between these results and the laboratory observations will be made.

APPARATUS AND DIAGNOSTICS

The apparatus used for the laboratory experiments allows for a liquid layer of variable depth to be established between two aluminum walls located 30 mm apart. Temperature-controlled water is circulated through the endwalls to establish isothermal conditions of T_H and $T_C < T_H$; these are measured with the use of thermocouples embedded in these endwalls and are used in the computation of the Marangoni number $Ma = \gamma \Delta T d^2 / \mu \kappa L$. In this expression, $\Delta T = T_H - T_C$ is the driving horizontal temperature difference, μ is the dynamic viscosity coefficient and d and L are the depth and length (L = 30 mm), respectively, defined in Fig. 1.

The layer is constrained laterally by two Plexiglas walls positioned 50 mm apart; the Plexiglas provides for a thermal condition approximating an adiabatic wall. The meniscus is pinned around its entire perimeter by having a sharp lip machined into the device. The horizontal surfaces of the lip are coated, prior to each set of experiments with a fluorinert compound which resists the wetting of these surfaces by the silicone oil (ν = 1 cS, corresponding to Pr = 13.93) used as the test liquid. Pinning the meniscus in this manner allows for a flat interface and well-defined layer depth. This is in contrast to earlier, related experiments by Villers and Platten (8) which appeared to make no apparent attempt to pin the meniscus. Schwabe *et al.* (9) conducted experiments in both rectangular and annular geometries; in the rectangular case, the meniscus appears to be pinned as in the present experiments. The depth is controlled by utilizing a false bottom of thick Plexiglas supported on three micrometers, allowing accurate positioning and depth control. Silicone oil also occupies a reservoir beneath the false bottom so that leakage through the bottom is not of concern in these experiments; this reservoir plays no role in the dynamics of the flow. A photograph of the apparatus is shown as Fig. 2; the view is similar to the sketch in Fig. 1, but from an angle above the horizontal.

Flow visualization experiments have been performed to characterize the various flow regimes in Ma–Bo_D space. Two types of flow visualization have been employed. In the first type of experiment, the layer is seeded with polystyrene spheres of sizes in the range 1.5 - 15 μm. A light sheet from an argon-ion laser is used to illuminate an x–y plane (See Fig. 1) of the flow and the particles are observed with either a digital camera and video recorder or with a still camera capable of taking time-exposure photographs. The second type of flow visualization employs a shadowgraphic technique. A collimated light source is used to illuminate the layer through one sidewall and the flow is observed through the other, i.e., in the z–direction of Fig. 1. The effect is therefore integrated across the layer and the images do not subject themselves to a simple interpretation (the patterns are representative of the second derivative of the density, or alternately, the second derivative of temperature). However, the technique appears to be very sensitive in detecting changes in flow structure and the onset of time dependence.

In addition to the flow-visualization work, various steady-flow states where characterized quantitatively using laser-Doppler velocimetry to map out the velocity fields for both steady, unicellular and steady, multicellular convection. These results are reported in the paper by Riley and Neitzel (10)

The primary interest in these experiments is in identifying the boundary associated with the onset of oscillatory thermocapillary convection, since this is the regime in which the control strategy will be implemented. Moreover, it is of interest to determine if there are regions in Ma–Bo_D space which exhibit a transition directly from steady, unicellular convection [the Smith and Davis (6) return-flow basic state] to oscillatory convection, in line with the Smith and Davis theory. It might be expected that the likelihood of this occurrence increases with decreasing Bo_D, since the calculations of Smith and Davis were performed assuming zero gravity. We shall see from the results that this is the case.

RESULTS

As just mentioned, the principal aim of these first experiments was to identify regions of Ma–Bo_D space which are likely to exhibit a transition directly from the steady basic state to oscillatory thermocapillary convection. The results of these experiments for a single silicone oil with Pr = 13.93 are shown in Fig. 3. It can be seen that such a transition occurs for Bond numbers in the range $0.075 < Bo_D < 0.2$. For Bond numbers above this range, the first transition from the steady basic state is to a state of steady, multicellular convection. Fig. 4 shows a comparison between a streak photograph and a shadowgraph for a case of this type, corresponding to (Ma, Bo_D) = (1350, 0.57). This value of Ma is significantly above the value (Ma = 680) at which the transition to steady, multicellular convection takes place for this Bond number. For a relatively deep layer such as seen in Fig. 4 (d = 2.0 mm), the multicellular structure nearly fills the entire layer; for smaller depths, the co-rotating cells shrink in size and are difficult to observe from the streak photographs, while the shadowgraphs still show a significantly distorted shape such as those seen here.

Fig. 5 is a photograph of the shadowgraphic image observed for a state which has undergone a transition directly to an oscillatory mode. This case corresponds to a layer depth of d = 1.0 mm with (Ma, Bo_D) = (460, 0.14), which is just slightly above the transition value of Ma = 455 for this Bo_D; in this regime, the transition to oscillatory convection is very sharp. The pattern seen here propagates to the left (toward the hot wall) in a very regular manner with a well-defined speed. It is the degree of this regularity, combined with the spatial nature of the instability, which makes it a candidate for active control and oscillation suppression.

Finally, it is worthwhile to examine the results of stability computations based on the Smith and Davis (6) theory with the inclusion of buoyancy. Fig. 6 shows the Marangoni number and wave speed as a function of wavenumber for the case of Bo_D = 0.50. The theoretical results reported here considered two-dimensional disturbances for simplicity. For Prandtl numbers in the range of the oil used in these experiments, the linear-theory Marangoni numbers are nearly indistinguishable for 2-D and oblique waves. The value of Ma_L corresponding to the minimum of the solid curve has an associated wave speed which yields waves propagating against the direction of the basic-state free surface. One observes from this graph that there does exist a wavenumber for which the wave speed is zero, possibly corresponding to a steady, multicellular mode. Fig. 7 shows the behavior of Ma_L and the Marangoni number corresponding to this zero-wave-speed value as a function of Bond number. At a value of Bo_D = 0.75, the critical state corresponds to one with zero phase speed, as compared to the occurrence of steady, multicellular states at $Bo_D \approx 0.2$ in the experiments.

One possible basis for differences in the magnitudes of the Marangoni numbers determined by experiment and theory is due to the fact that the theoretical calculations assume a basic state with a linear temperature gradient which is used to evaluate Ma. In the experiments, this gradient is approximated by $\Delta T/L$, which is much larger than the shallow gradient in the middle of the layer. Encouraging is the fact that the Smith and Davis, zero-gravity stability limit (indicated on Fig. 3 by an arrow) is in good agreement with the experimentally determined result for small Bond number, although the degree of this agreement is in need of further interpretation, given the statement in the previous sentence. Mid-layer surface-temperature gradients will be measured during the next phase of the research.

DISCUSSION AND FUTURE WORK

An apparatus has been constructed and used to demonstrate the existence of oscillatory thermocapillary convection. The apparatus is designed to pin the meniscus around the entire perimeter so that a flat interface and well-defined depth may be achieved. Three flow regimes have been identified and a stability map constructed for a limited range of Ma–Bo_D space. On a portion of this plane, the transition to oscillatory thermocapillary convection is a sharp one and occurs directly from the steady, return-flow basic state without passing through a steady, multicellular state.

Now that a range of Bo_D has been identified in which the transition occurs from steady, unicellular thermocapillary convection to oscillatory thermocapillary convection, we shall begin to implement the proposed control strategy. This involves detecting the surface-temperature variations with the use of an infrared camera and then actively supplying heat to regions of negative disturbance temperature to homogenize the free-surface temperature. The heat is to be supplied with a carbon-dioxide laser, making use of the properties of silicone oil determine by Pline (11) in support of the Surface-Tension-Driven Convection Experiment (STDCE).flown on the USML-1 Shuttle mission.

The control strategy to be employed is envisioned to utilize feed-forward control to detect the presence of waves at one spatial location and then suppress them at a distance downstream of this point, where by downstream, we refer to the direction of propagation.. If the instability mechanism postulated by Smith (7) is correct and if the flow being observed is indeed a hydrothermal-wave instability, then this strategy should result in the successful suppression of oscillatory convection downstream of the heating location.

ACKNOWLEDGMENT

The experiments and modifications to the Smith and Davis theory reported on herein have been performed by Mr. R. J. Riley as part of his doctoral research.

REFERENCES

1. H.C. Gatos, in G.E. Rindone, (ed.) Materials Processing in the Reduced Gravity Environment of Space, Elsevier, 1982,

2. Y. Shen, *et al.*, J. Fluid Mech., 217 (1990), 639-660.

3. G.P. Neitzel, *et al.*, Phys. Fluids A, 3 (1991), 2841-2846.

4. G.P. Neitzel, *et al.*, Phys. Fluids A, 5 (1993), 108-114.

5. H. Kuhlmann and H. Rath, J. Fluid Mech., 247 (1993), 247-274.

6. M.K. Smith and S.H. Davis, J. Fluid Mech., 132 (1983), 119-144.

7. M.K. Smith, Phys. Fluids, 29 (1986), 3182-3186.

8. D. Villers and J.K. Platten, J. Fluid Mech., 224 (1992), 487-510.

9. D. Schwabe, *et al.*, Phys. Fluids A, 4 (1992), 2368-2381.

10. R.J. Riley and G.P. Neitzel, in G.P. Neitzel and M.K. Smith, (ed.) Surface-Tension-Driven Flows, ASME, 1993,

11. A.D. Pline, NASA-TM 101353 (1989), NASA Lewis Research Center.

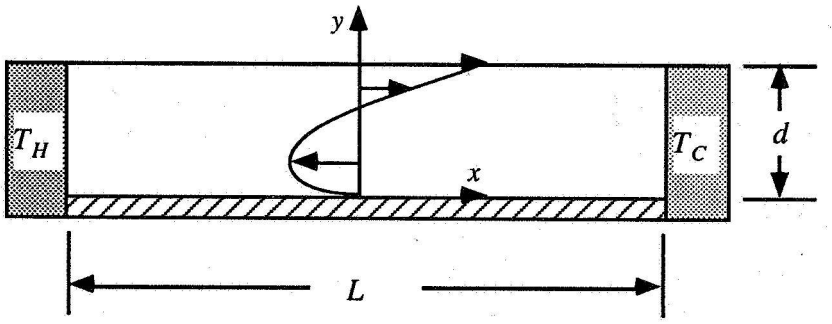

Thermocapillary convection return-flow basic state in a layer of finite length.

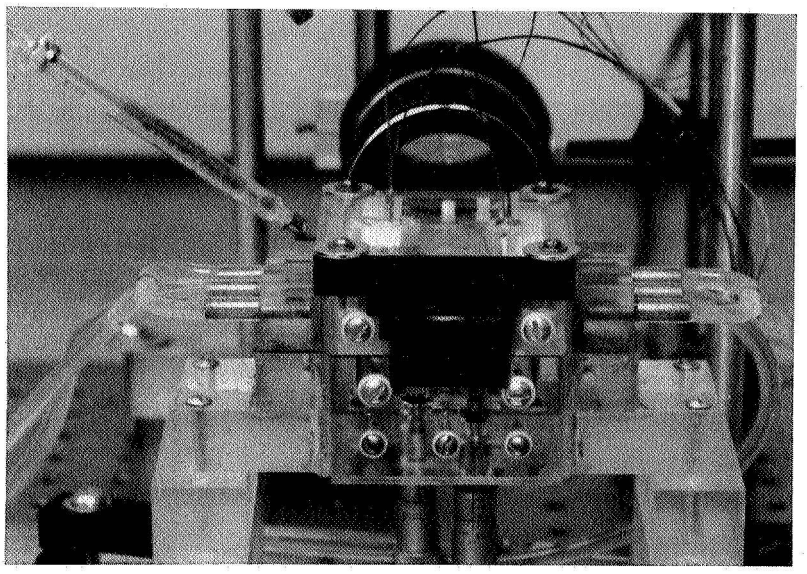

Fig. 2. Photograph of the experimental apparatus.

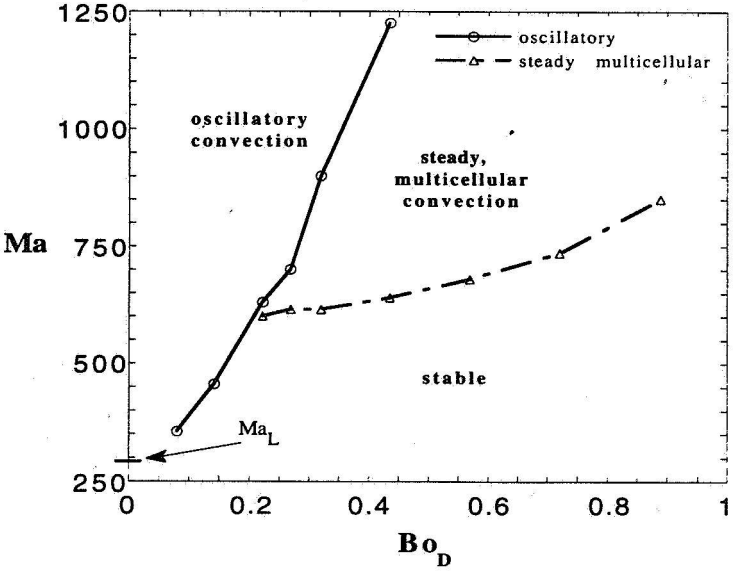

Fig. 3. Experimental results for 1 cS silicone oil with Pr = 13.93.

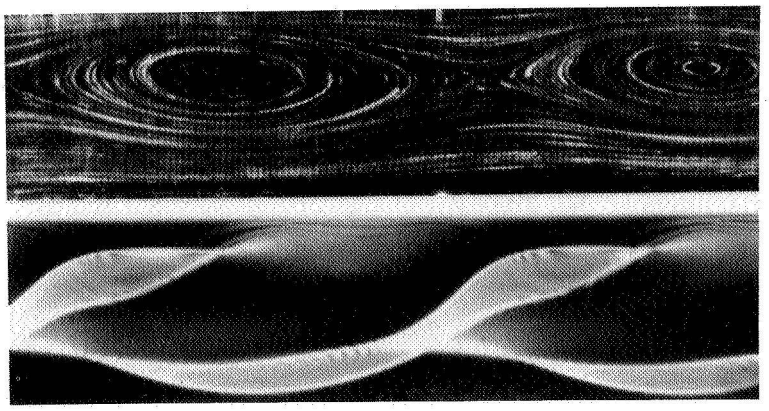

Fig. 4. Streak photograph and shadowgraph for a steady, multicellular case with $d = 2.0$ mm and $(Ma, Bo_D) = (1350, 0.57)$.

Fig. 5. Shadowgraph for an oscillatory case with $d = 1.0$ mm and $(Ma, Bo_D) = (460, 0.14)$.

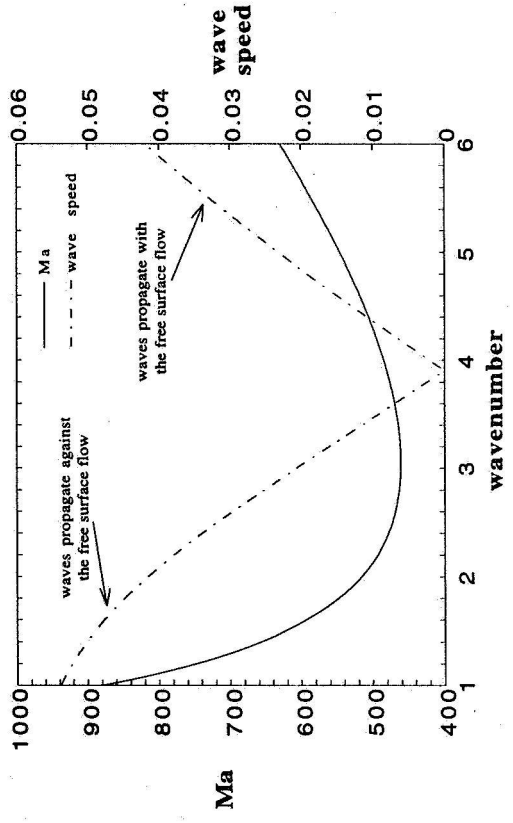

Fig. 6. Linear-stability calculations versus wavenumber.

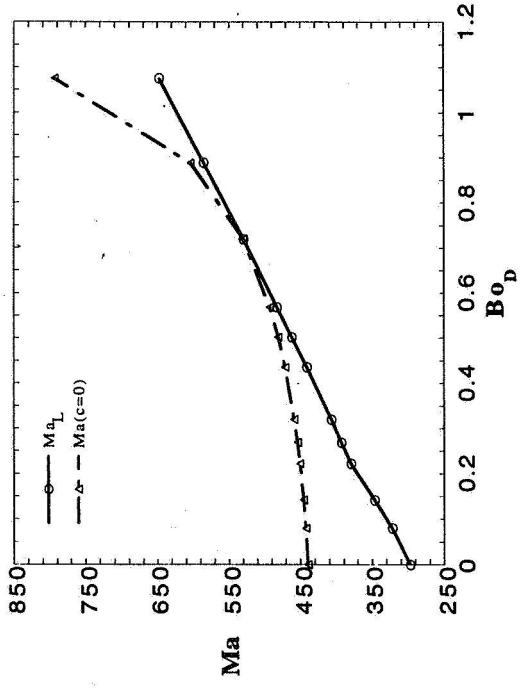

Fig. 7. Linear-stability results including buoyancy.